

## **Hydrogeochemical Characteristics and Evolution of Groundwater at the Ras Sudr-Abu Zenima Area, Southwest Sinai, Egypt**

**Anwar A. El-Fiky**

*Hydrogeology Department, Faculty of Earth Sciences,  
King Abdulaziz University,  
P.O. Box: 80206 Jeddah, 21589, Saudi Arabia*

Received: 17/1/2009

Accepted: 14/10/2009

*Abstract.* The hydrogeochemical and isotopic data of groundwaters of the different aquifers of the Ras Sudr-Abu Zenima area, southwest Sinai, Egypt were examined to determine the main factors controlling the groundwater chemistry and salinity as well as its hydrogeochemical evolution. Groundwater occurs in different water-bearing formations belonging to Quaternary, Neogene, Upper Cretaceous, and Paleozoic. Different geochemical interpretation methods were used to identify the geochemical characteristics. Groundwater of the coastal Quaternary alluvial aquifer has the highest salinity values (2739-7040 mg/l) in the study area due to the impact of seawater and agricultural activities. Piper diagram showed that Cl and SO<sub>4</sub> are the dominant anions, whereas Na is the most dominant cation, where it is sometimes replaced by Ca and/or Mg in the hydrochemical facies of the groundwaters. Durov diagram plot revealed that the groundwater has been evolved from Ca-HCO<sub>3</sub> recharge water through mixing with the pre-existing groundwater to give mixed water of Mg-SO<sub>4</sub> and Mg-Cl types that eventually reached a final stage of evolution represented by a Na-Cl water type. Different ionic ratios revealed the impact of seawater and marine aerosols on the hydrochemical composition of groundwater of the Quaternary aquifer. Dissolution of carbonate and sulfate minerals in the aquifer matrices and recharge areas as well as cation exchange are shown to modify the concentration of ions in groundwater. Groundwater-mineral equilibria showed the prevailing dissolution-precipitation reactions in the groundwater. The groundwaters are depleted in <sup>2</sup>H and <sup>18</sup>O and displayed an isotopic signature close to that of meteoric water with d-excess values indicating present-day precipitation over the region and

reflect the contribution of vapour masses from Mediterranean origin. The isotopic features suggest that most of the groundwaters at the study area result from mixing between recent recharge and an older component recharged under climatic conditions cooler than at present. Moreover, groundwaters from the Cambrian and Carboniferous water-bearing formations show  $\delta$ -excess values of 13.9 and 10.96‰, respectively, which indicates that older component of recharge is prevailing than the recent one. Isotopic signature of groundwater from the Quaternary aquifer indicated seawater contribution.

*Keywords:* Hydrogeochemistry, Groundwater, Ionic ratios, Sinai, Egypt.

## Introduction

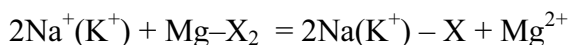
During the last decades groundwater exploitation in the Sinai Peninsula has increased dramatically, mainly due to an increase in irrigated agriculture, tourism and industry. To meet the needs of drinking water for future generations, sustainable watershed management is essential for drinking water supply especially in semiarid areas, and requires a more detailed knowledge about recharge processes. In many cases conventional hydrogeochemical studies are not sufficient to characterize groundwater hydrodynamics or to detect recharge areas and source areas of recharged water. Since the isotopic composition of O and H in groundwater does not change as a result of rock–water interactions at low temperatures, it provides a helpful means to bridge this knowledge gap (*e.g.* Sidle, 1998). The application of isotope-based methods has become well established for water resource assessment, development and management in the hydrological sciences, and is now an integral part of many water quality and environmental studies (Clark and Fritz, 1999; and Cook and Herczeg, 1999). Several studies using hydrochemistry and stable isotopes of water have already been realized to characterize hydrogeochemistry and recharge processes in similar hydrogeologic environments (Marfia *et al.*, 2003; Long and Putnam, 2004; Barbieri *et al.*, 2005)

The study area extends from Ras Sudr to Abu Zenima along the Gulf of Suez, southwest Sinai, Egypt. It exhibits important and well developed sedimentary drainage basins that are draining surface runoff from the elevated tableland (El-Tih plateau) to the Gulf of Suez. Wadi Sudr, Wadi Wardan and Wadi Gharandal-Wadi Abu Gaada (a main tributary of Wadi Gharandal) are the main drainage basins in the study area and contain different important aquifer systems: 1) The Quaternary

alluvial aquifer system, which occupies the downstream parts of these basins, 2) The Neogene aquifer system is represented by the Miocene water-bearing formations that are located at the middle part of Wadi Sudr and upper part of Wadi Gharandal, 3) The karstified limestone aquifer of Upper Cretaceous-Eocene is the most important aquifer system at the upstream parts of Wadi Sudr and Wadi Abu Gaada, 4) The Lower Cretaceous Nubian sandstone aquifer system is exposed at the eastern part of Wadi Abu Gaada, 5). The Paleozoic water-bearing formations lying to the east of Abu Zenima along the scarp of El-Tih Plateau and are represented by the Arabah Formation of Cambrian age and the Abu Thora Formation of Lower Carboniferous.

Groundwater in the coastal areas of the downstream parts of the previously mentioned drainage basin is vulnerable to salinization by seawater, which can make it unfit for drinking or agricultural use. Moreover, groundwater salinization can be increased by natural processes and anthropogenic factors (Herrera *et al.*, 2008; Capaccionia *et al.*, 2005; Custodio, 1987; El Baruni, 1995; El Mandour *et al.*, 2007; Ferrara and Pappalardo, 2004; Grassi and Netti, 2000; Lambrakis *et al.*, 1997; and Petalas and Diamantis, 1999). Generally, fresh groundwater that is not affected by pollution is characterized by low values of EC and Ca–Mg–HCO<sub>3</sub> water type. The latter represents freshwater that has recently infiltrated into the zone of recharge, while the EC shows a gradual increase from the uplands recharge areas towards the lowlands discharge areas. Along the coastline, high values of EC are usually attributed to salinization by seawater intrusion (Stamatis and Voudouris, 2003). According to Appelo and Postma (2005), some water types characterize salt groundwater: Na–Cl dominant type, Ca–Cl, indicating the seawater intrusion process, and Na–Mg–Cl–SO<sub>4</sub>, representing a mixed water type. Water–rock interaction can alter groundwater; high-SO<sub>4</sub> concentrations can be associated with the dissolution of gypsum, which is commonly encountered along the Gulf of Suez. Cation exchange is another factor modifying groundwater quality and is one of the most important geochemical processes taking place in aquifers. In coastal aquifers, where the relationship between seawater and fresh water is complex, cation exchange contributes significantly to the final composition of the groundwater. In detrital sedimentary aquifers, cation exchange is one of the most important geochemical processes of seawater intrusion (Cardona *et al.*, 2004). The ion exchange reactions of Na and

Ca often occur when seawater intrudes fresh groundwater. The characteristic cation-exchange process that takes place when seawater intrudes a coastal fresh water aquifer is (Appelo and Postma, 2005):



where, X represents ion exchange sites in aquifer materials. When fresh groundwaters flush out saline groundwaters, the reverse reactions occur.

The objective of this study was the investigation of the hydrogeochemical evolution and the recharge processes of groundwater in the main basins subjected to increasing agricultural exploitation. The stable isotope ratios of H and O and concentrations of major and minor ions of groundwater are essential in understanding geochemical processes affecting water quality. The results of this study may contribute to the optimization of water resources management.

### Geological Setting

The Sinai Peninsula occupies a portion of the foreland shelf of the Arabo-Nubian massif that dips gradually northward toward the Mediterranean Sea (Said, 1962). Its morphology, stratigraphy, and structures are strongly interrelated and have a great bearing on the groundwater potential (Issar *et al.*, 1972). The sedimentary succession encountered in Sinai includes different types of sediments that were deposited on a predominately shallow platform and range in age from Cambrian to Recent (Fig. 1). Said (1962) divided the sedimentary sequence of Sinai into three divisions: (1) the lower clastic division, which overlies the Precambrian basement rocks and extends to the Lower Cretaceous Nubian Sandstone; (2) the middle calcareous division, which ranges in age from Cenomanian to Eocene; and (3) the upper clastic division of Neogene to Holocene age.

In Western Sinai, the Nubian sandstones (Issawi, 1973) rest on Carboniferous limestone. These rocks consist of continental sandstones with thin beds of marine limestones, and marls. This mainly sandy unit corresponds essentially to continental deposits (Schütz, 1994). The pre-rift marine formations that cover the Nubian sandstones comprise a thick Cretaceous to Eocene succession of marine deposits that is subsequently overlain by conglomerate and evaporite synrift series in the center of the

trough. Salem (1995) indicated that the exposed sandstones in southwest Sinai marginal to the Gulf of Suez are entirely or partly of Carboniferous age. This sandstone unit is represented by medium to coarse grained sandstones. Omara (1967) suggested a Visean age for this unit, while Said (1971) assigned a Permian age for the upper parts and Late Carboniferous for the lower parts of this unit. These sandstones are exposed along the scarp of Gebel El-Tih. The Cretaceous rocks are widely distributed in Sinai. They are well exposed along the eastern and the western side of the Gulf of Suez as well as at the northern part of Sinai.

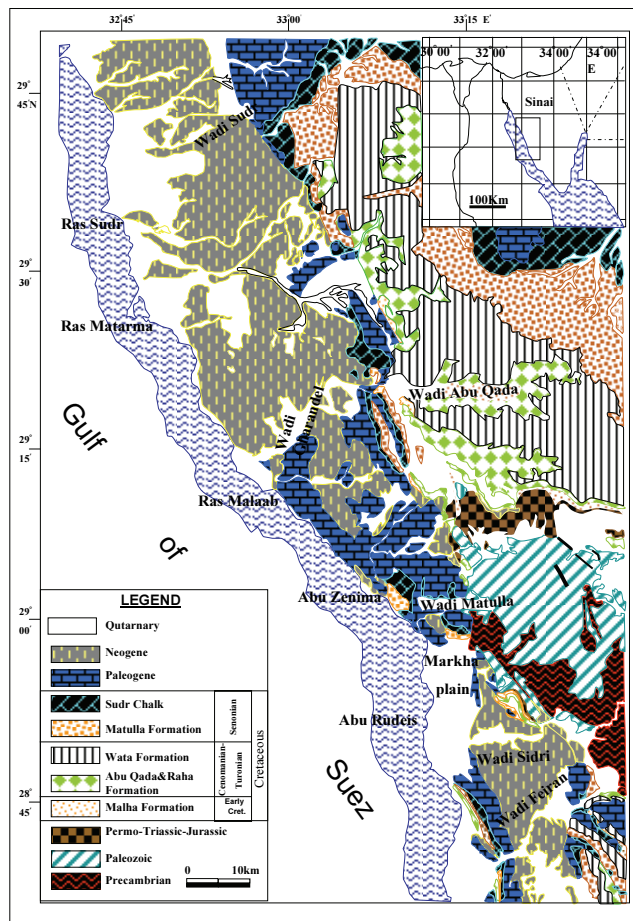


Fig. 1. Geological map of southwest Sinai (modified from Conoco, 1987).

The sedimentary sequence exposed at the study area includes a wide range of geologic ages. This sequence begins at the lower part with Upper Cretaceous sequence (Cenomanian – Maastrichtian), that is overlain by the calcareous Eocene sediments and the sequence is ended with the upper clastic rocks of Neogene to Holocene. Older rocks belonging to the Nubian facies are exposed to the east of Abu Zenima along the scarp of Gebel El-Tih and are represented by the Arabah Formation of Cambrian age and the Abu Thora Formation of Lower Carboniferous. The Arabah Formation is composed of varicolored, laminated sandstone with sandy clay and ferruginous bands. The Abu Thora Formation is made up of sandstone with intercalations of carbonaceous clay.

The Upper Cretaceous sequence comprises five formations (Ghorab, 1961); namely from youngest to oldest: the Sudr Chalk (Campanian – Maastrichtian), the Matulla (Coniacian – Santonian), the Wata (Turonian), the Abu Qada and the Raha (Cenomanian). The Raha Formation overlies the Nubian sandstone (Malha Formation) of the Lower Cretaceous and underlies the Abu Qada Formation. The Abu Qada Formation represents the Turonian sediments above the inner sublittoral deposits of the Cenomanian. The Wata Formation is deposited above the Raha Formation. The Matulla Formation, which overlies the Wata Formation, consists mainly of limestones, marls commonly alternating with shales, sandstones, shaley limestones and siliceous limestones. This Upper Cretaceous sequence is topped by the Sudr Formation that is composed mainly of chalk, partly changing to marls or argillaceous to crystalline limestone. The Upper Cretaceous sequence is unconformably overlain by calcareous Eocene sediments (limestone, chert, marl and shale).

The Eocene sequence is classified into four formations; the Thebes Formation (Lower Eocene), the Minia Formation (Lower Eocene), the Darat Formation (Lower-Middle Eocene) and the Tanka Formation (Upper Eocene). The Eocene sequence is overlain by the Oligocene Abu Zenima Formation that is composed of sandstone and siliceous conglomerate. Esna Formation of Paleocene to Lower Eocene age locally underlies the Thebes Formation.

The Miocene sequence exposed at the study area is classified into two main groups: the Early Miocene Gharandal Group and the Middle

Miocene Ras Malaab or Evaporite Group (Egyptian General Petroleum Corporation, EGPC, 1964; Gawad *et al.*, 1986). The lower Gharandal Group comprises from base to top the Nukhul, Rudeis and Kareem formations. The Gharandal Group is made up of clastics, marl and carbonates, partly reefal. The Ras Malaab Group is predominantly composed of evaporites and intercalated shale.

The structural pattern of west central Sinai shows that faulting is much more pronounced than folding. The region underwent minor folding in the Late Palaeozoic (Abdallah *et al.*, 1992) and then rifting of part of the Gulf of Suez, which began in the Early Miocene and continues to the present (Purser *et al.*, 1993). Faults are the result of successive movements which affected the area in different ages. Said (1962) proposed the age of this faulting as Oligocene and/or Early Miocene. However, El Gammal (1984) showed that the faulting has taken place periodically since the Late Paleozoic, increased in intensity and areal extension progressively and reached its climax in the Oligo-Miocene period.

### **Hydrogeological Setting**

South Sinai is characterized by arid climatological conditions. Values of the average monthly climatic elements recorded at the Ras Sudr meteorological station (Egyptian Meteorological Authority) for the period 1978-1993, show that the highest average monthly maximum temperature is recorded in July (35.3°C) and the lowest average monthly minimum temperature is recorded in December (6.5°C). Highest rates of evaporation are recorded in June, where the average value was 15.70 mm. Rainfall is frequently occurring during the autumn (October, November, and December) and winter (January, February, and March) seasons. The highest average monthly value of rainfall is recorded in January (4.11 mm). Rainfall may cause severe flash floods, which have noticeable destructive impact on the asphaltic roads and residential areas. The study area is characterized by the occurrence of well-developed surface drainage system that debouches into the Gulf of Suez. Wadi Sudr, Wadi Wardan, and Wadi Gharandal are the main drainage basins in the study area.

Figure 2 shows locations of the investigated water points at the Sudr-Abu Zenima area. At this area, groundwater occurs mainly under

unconfined conditions in different water-bearing formations of varying lithologies and ages as follows:

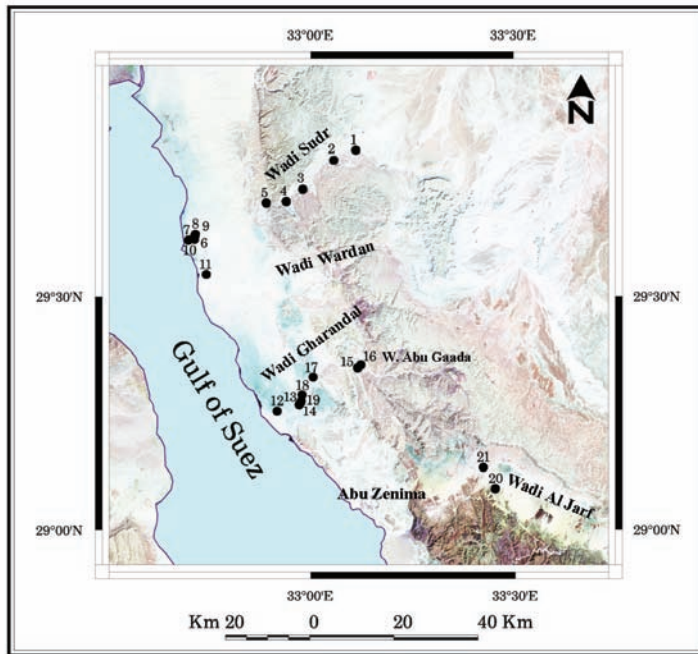


Fig. 2. Location map of the investigated water points at the Sudr-Abu Zenima area.

### *The Quaternary Alluvial Aquifer*

It lies in the downstream parts of Wadi Sudr, Wadi Wardan, and Wadi Gharandal. It is composed of alluvial deposits, which are made up of gravel intercalated with varicolored clay and calcareous sandstone (Hassanein, 1989; Misak *et al.*, 1995). The groundwater in the downstream parts of Wadi Sudr and Wadi Wardan (water points 6, 7, 8, 9, 10, and 11) is encountered at depths ranging from 3.5 m near the coastline to 17.5 m to the east. El Sayed *et al.* (1999) showed that the groundwater flows generally from east towards west, where the Gulf of Suez represents the natural discharge area of the Quaternary aquifer, with a hydraulic gradient ranges between 0.002 and 0.01. High hydraulic gradient is associated with over-pumping of groundwater, which is extracted mainly for irrigation. This aquifer has high transmissivity values, which reach up to 5068 m<sup>2</sup>/day and a specific yield of 0.042 (El



Sayed *et al.*, 1999). These values indicate that the Quaternary aquifer has high potentiality and it is considered as the most productive aquifer in the Gulf of Suez Rift Province (Mills and Shata, 1989).

Westwards of the outcrops of the Neogene beds in Wadi Gharandal, the Quaternary alluvial deposits were brought in front of the Neogene beds of the Gharandal Formation along a NW-SE fault, where groundwater is encountered at shallow depths. Moreover, water table intersects the ground surface, where groundwater issues as a depression spring (water point no. 12 or Ain Gharandal) close to Sudr-Abu Zenima Highway. The Quaternary alluvial aquifer is a highly productive one and its groundwater is used mainly for irrigation.

### ***The Neogene Water-Bearing Formations***

In the middle and upper parts of Wadi Gharandal, the Neogene water-bearing formation is represented by the Gharandal Formation, which is composed of conglomerate, gravel and sand beds dipping towards west and southwest with a dip angle ranging between 30 and 35° (Abdel-Mogheeth *et al.*, 1985). The Gharandal Formation forms the main aquifer in the upper and middle parts of Wadi Gharandal, where the groundwater occurs at depths varying from 18 to 23 m below the ground surface (water points 13, 14, 15, 17, 18, and 19 in Wadi Gharandal). The Gharandal Formation is dissected by a number of basaltic dykes that influence groundwater occurrences. In Wadi Sudr, the Neogene water-bearing formation is represented by the Lower Miocene Sumar Formation, which is composed of yellow marly limestone with conglomerate at the base. Groundwater is issued naturally from this formation at Ain Abu Garad (water point no. 5).

### ***The Upper Cretaceous-Eocene Highly Fractured and Karstified Limestone Aquifer***

This aquifer is located at the upstream parts of Wadi Sudr, Wadi Wardan and Wadi Abu Gaada. It constitutes the most important and productive aquifer at the eastern parts of the dissected tableland (El-Tih Plateau). This aquifer is continuously recharged by rainfall, where water seepage is facilitated by the fractured and karstified nature of limestone (Abdel Mogheeth *et al.*, 1985, Misak *et al.*, 1995). The groundwater issues naturally through a number of perennial springs, which are

structurally and lithologically controlled (e.g. Ain Sudr, Ain Abu Rejem, Ain Henaik, Ain Um Gorf represented by water points from 1 to 4 in Wadi Sudr, and water point no. 16 in the lower part of Wadi Abu Gaada).

### ***The Lower Cretaceous Sandstone Aquifer***

The Lower Cretaceous Nubian Sandstone aquifer in the Sinai Peninsula is an extension of the sandstone formation of the African shield that underlies Egypt and Libya and that extends westward through the Sahara Desert (Melloul 1995). The aquifer consists of alternating beds of sandstone and shale in the central and southern Sinai and changes in facies to carbonate and shale north of the El-Maghara–El-Halal Mountains folded zone (Water Resources Research Institute and Japan International Cooperation Agency 1999). The carbonate rocks overlying the Nubian Sandstone complex display karst features locally, and are recharged by upwards leakage from the underlying major aquifer.

In the study area, this water-bearing formation (Nubian sandstone) is represented by the Malha Formation of Aptian-Albian age and composed of sandstone with subordinate interbeds of sandy siltstone and claystone and kaolinitic pockets. It is exposed at the eastern part of Wadi Abu Gaada, where it is occasionally exposed on its floor and becomes overlain by younger formations to the west.

### ***The Paleozoic Water-Bearing Formations***

These formations belong to the Nubian facies and are exposed to the east of Abu Zenima along the scarp of Gebel El-Tih and are represented by the Abu Thora Formation of Lower Carboniferous age (water point no. 21 or Rocknah well-3) and the Arabah Formation of Cambrian age (water point no. 20 or Seeh large diameter well). The Abu Thora Formation is made up of sandstone with intercalations of carbonaceous clay. The Arabah Formation is composed of varicolored, laminated sandstone with sandy clay and ferruginous bands. Groundwater occurs in these formations under unconfined conditions and is encountered at a depth of 55.6 m at Rocknah well, where groundwater is pumped with a discharge rate of 35 m<sup>3</sup>/h. Groundwater is also encountered at a depth of 20.8 m below the ground surface at Seeh well. The groundwater from these sandstone formations is of low salinity that is suitable for drinking and agricultural purposes.

## Methods of the Study

### *Sampling and Analysis*

Hydrogeological information were gathered from a sampling plan set up in February 2005. Twenty one wells and springs were sampled from the different basins at the Ras Sudr-Abu Zenima area, southwest Sinai, Egypt (Fig. 2). Chemical and isotopic data of the Red Sea water (Wilson, 1975; and Craig, 1969) were used in the present study. The temperature ( $T^{\circ}C$ ), pH, and electrical conductivity (EC) were measured in the field. Chemical analyses of major ions (Ca, Mg, Na, K,  $HCO_3$ ,  $SO_4$ , and Cl) and Boron (B) were carried out at the laboratory of the Department of Environmental Sciences, Faculty of Science, Alexandria University, Egypt, using standard analytical procedures (American Public Health Association APHA, 1998). Calcium, Mg,  $HCO_3$  and Cl were determined by titrimetric methods. Flame photometry was used to measure the concentrations of Na and K. Sulfate was determined using the turbidimetric method. Boron was analyzed spectrophotometrically using the carmine method. Bromide (Br) and iodide (I) were determined using ion selective electrode Ionometer, Orion-930 at the Desert Research Center, Cairo. The analytical precision for measurement of ions was determined by calculating the ionic balance error, which falls within the acceptable limits of  $\pm 5\%$ . Stable isotopes of oxygen and hydrogen ( $^{18}O$ ,  $^2H$  or D) were performed at the National Center, U.S. Geological Survey, Reston, USA. Hydrogen isotope ratio analyses have been performed using a hydrogen equilibration technique similar to Coplen *et al.* (1991). Water samples were measured for  $\delta^{18}O$  using the  $CO_2$  equilibration technique of Epstein and Mayeda (1953), which has been automated. Analytical precision was  $\pm 0.1\%$  for  $^{18}O$  and  $\pm 1\%$  for  $^2H$ . Isotopic compositions were reported in  $\%$  deviation from isotopic standard reference material, VSMOW (Vienna Standard Mean Ocean Water) using the conventional  $\delta$  notation where:

$$\delta (\%) = [(R_{\text{sample}} - R_{\text{standard}})/R_{\text{standard}}] \times 10^3$$

where R is the ratio of the heavy to light isotope abundances.

Saturation indices of some common minerals were calculated using the program PHREEQC (Parkhurst and Appelo, 1999) interfaced with AquaChem Version 5.

## Results and Discussion

### *Chemical Characterization*

Chemical composition of the groundwater samples collected from different water-bearing formations during February 2005 are summarized in Table 1, and plotted on Piper and Durov diagrams (Fig. 3 and 4).

#### *Groundwater from the Quaternary Alluvial Aquifer*

Groundwaters from the downstream parts of Wadi Sudr, Wadi Wardan and Wadi Gharandal (water points from 6 to 12) have the highest salinity values throughout the study area. The groundwaters have pH values ranging from 7.11 to 7.37 indicating a near neutral pH. TDS values range from 2739 (water point # 9 in the downstream part of Wadi Sudr) to 7040 mg/l (water point 12 or Ain Gharandal). These values indicate the brackish nature of these groundwaters, which is possibly attributed to the nature of the alluvial deposits which are rich in soluble minerals in addition to agricultural return flow that causes leaching of soluble salts precipitated in the soil zone under the high evaporation rate. Mixing with the underlying dense salt water is another source of salinization of groundwaters from the coastal Quaternary aquifer, mostly caused by overpumping. Sodium is the dominant cation in the chemical facies of most groundwater samples, followed by Mg and Ca (Table 2).

One sample (# 9) shows different cation dominance, where the dominant cations in the chemical facies are Mg and Ca. Three samples (# 8, 10 and 12) have Na as the dominant cation where Ca and Mg are not represented in their chemical facies. Distribution of the groundwater samples from the Quaternary aquifer in the Piper diagram (Fig. 3) shows that these samples are characterized by the dominance of Cl + SO<sub>4</sub> over HCO<sub>3</sub>. Three samples (8, 10 and 12) show dominance of Na over Ca + Mg. The rest of the samples show dominance of Ca + Mg over Na. Sample # 12 (Ain Gharandal) is the closest sample to the point representing seawater indicating possible mixing with seawater.

**Table 1. Hydrochemical and isotopic parameters of the groundwater from the different water-bearing formations in southwest Sinai, Egypt. (Chemical parameters in mg/l)**

#	Sample Name	Geology	pH	T°C	EC (µS/cm)	TDS (mg/l)	Ca	Mg	Na	K	HCO <sub>3</sub>	SO <sub>4</sub>	Cl	B	Br	I	<sup>18</sup> O (‰)	<sup>2</sup> H (‰)	d- excess
1	Ain Sudr	U. Cretaceous	7.86	10.0	3670	2349	73.2	139.9	510	5	319.8	500	736	0.92	2.2	0.00200	-5.9	-29.3	17.9
2	Ain Abu Rejem	U. Cretaceous	7.43	16.5	3820	2445	182.2	117.8	460	9.5	270.1	610	743	0.99	2.3	0.00190	-6.2	-33.2	16.4
3	Ain Henaik	U. Cretaceous	8.12	14.0	840	538	72.9	24.6	60	5	127.9	138	118	2.22	0.4	0.00032	-5.7	-31.7	13.9
4	Ain Um Gorf	U. Cretaceous	8.33	19.5	1500	960	101.0	56.5	124	9	149.2	290	230	0.79	0.8	0.00060	-5.1	-29.6	11.2
5	Ain Abu Garad	L. Miocene	7.75	17.6	1510	966	72.9	71.2	140	10	241.6	251	207	0.58	0.7	0.00056	-5.8	-31.8	14.6
6	DRC-1	Quaternary	7.33	22.7	6620	4237	404.8	274.9	540	5	184.8	960	1517	1.43	4.8	0.00410	-5.3	-25.1	17.3
7	DRC-2	Quaternary	7.37	20.6	6550	4192	404.8	250.4	570	5.5	156.3	900	1563	1.22	5.3	0.00430	---	---	---
8	WS-1	Quaternary	7.11	20.2	7880	5043	363.6	213.6	1010	9	213.2	1120	1839	2.31	5.9	0.00500	-5.1	-24.8	16
9	WS-2	Quaternary	7.20	17.8	4280	2739	303.6	208.6	250	6	85.3	1000	720	1.69	2.4	0.00190	---	---	---
10	WS-3	Quaternary	7.13	18.1	8400	5376	392.6	270.0	970	9	142.1	1180	2023	1.86	6.9	0.00550	---	---	---
11	WW-1	Quaternary	7.24	17.6	9910	6342	538.3	309.3	1080	15	213.6	1540	2207	1.86	7.4	0.00600	-5.2	-24.0	17.6
12	WGH-1	Quaternary	7.33	13.5	11000	7040	528.0	175.6	1680	35	283	1260	2849	1.99	10.0	0.00680	-3.49	-13.6	14.32
13	WGH-2	L. Miocene	7.28	20.0	3100	1984	219.0	93.3	290	22	246	714	483	1.28	1.6	0.00130	---	---	---
14	WGH-3	L. Miocene	7.31	17.5	2600	1664	115.0	131.6	235	19	132	650	389	1.25	1.2	0.00100	---	---	---
15	WGH-4	L. Miocene	7.65	23.0	1180	735	70.5	42.2	98	11	161	180	171	1.19	0.6	0.00045	-5.9	-31.6	15.6
16	WGH-5	U. Cretaceous	7.56	21.0	1000	640	40.8	53.3	90	11	160	220	141	1.18	0.5	0.00039	-6.7	-34.2	19.4
17	WGH-6	L. Miocene	7.36	20.5	2150	1376	81.7	97.8	210	18	177	452	342	1.24	1.2	0.00093	---	---	---
18	WGH-7	L. Miocene	7.32	21.0	2350	1504	100.2	102.2	212	17	172	558	332	1.23	0.9	0.00090	---	---	---
19	WGH-8	L. Miocene	7.48	19.0	3500	2240	219.0	122.2	275	24	189	916	443	1.27	1.5	0.00120	---	---	---
20	Seeh well	Cambrian	7.30	18.0	1450	928	63.1	66.7	140	12	160.6	290	236	1.20	0.8	0.00060	-6.2	-35.7	13.9
21	Rocknah well-3	Carboniferous	7.12	20.0	1300	832	55.7	40	155	11	143.4	200	220	1.20	0.7	0.00059	-5.72	-34.8	10.96
22	Red Sea water*				42,000	494	1553	1292.8	479	170	325.4	2321.3	5	81	0.06400	1.4**	7**		

WS: Wadi Sudr, WW: Wadi Wardan, WGH: Wadi Gharamdal, DRC: Desert Research Center, ---: not determined, \*: Wilson (1975), \*\*: Craig (1969)

Table 2. Hydrochemical facies of groundwater from the different water-bearing formations.

#	Sample Name	Geology	Hydrochemical Facies
1	Ain Sudr	Up. Cretaceous	Na-Mg-Cl
2	Ain Abu Rejem	Up. Cretaceous	Na-Cl-SO <sub>4</sub>
3	Ain Henaik	Up. Cretaceous	Ca-Na-Cl-SO <sub>4</sub>
4	Ain Um Gorf	Up. Cretaceous	Na-Ca-Mg-Cl-SO <sub>4</sub>
5	Ain Abu Garad	Lower Miocene	Na-Mg-Cl-SO <sub>4</sub>
6	DRC-1	Quaternary	Na-Mg-Ca-Cl-SO <sub>4</sub>
7	DRC-2	Quaternary	Na-Mg-Ca-Cl
8	WS-1	Quaternary	Na-Cl
9	WS-2	Quaternary	Mg-Ca-SO <sub>4</sub> -Cl
10	WS-3	Quaternary	Na-Cl
11	WW-1	Quaternary	Na-Cl-SO <sub>4</sub>
12	WGh-1	Quaternary	Na-Cl
13	WGh-2	Lower Miocene	Na-Ca-SO <sub>4</sub> -Cl
14	WGh-3	Lower Miocene	Mg-Na-SO <sub>4</sub> -Cl
15	WGh-4	Lower Miocene	Na-Ca-Mg-Cl-SO <sub>4</sub>
16	WGh-5	Up. Cretaceous	Mg-Na-SO <sub>4</sub> -Cl
17	WGh-6	Lower Miocene	Na-Mg-Cl-SO <sub>4</sub>
18	WGh-7	Lower Miocene	Na-Mg-SO <sub>4</sub> -Cl
19	WGh-8	Lower Miocene	Na-Ca-SO <sub>4</sub> -Cl
20	Seeh well	Cambrian	Na-Mg-Cl-SO <sub>4</sub>
21	Rocknah well-3	Carboniferous	Na-Cl-SO <sub>4</sub>

WS: Wadi Sudr, WW: Wadi Wardan, WGh: Wadi Gharandal, DRC: Desert Research Center

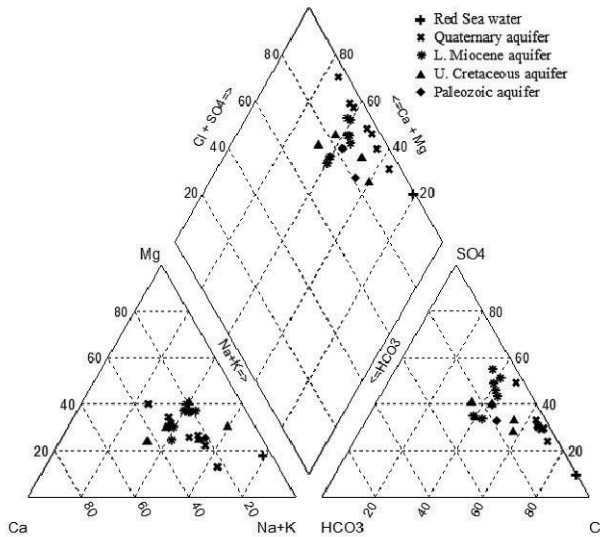
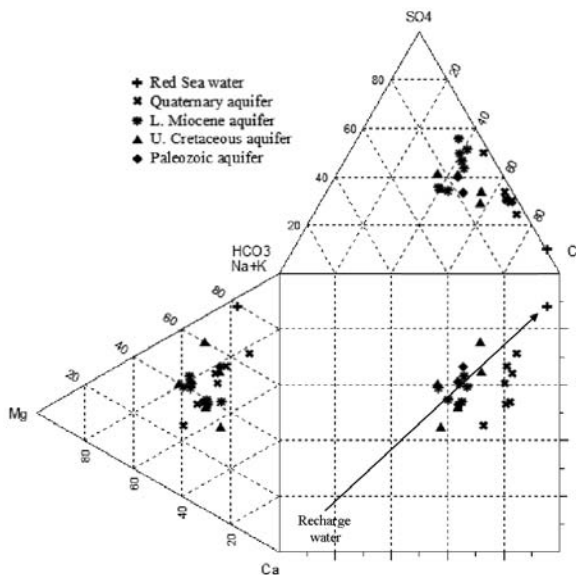


Fig. 3. Piper diagram plot of groundwater from the study area.

Presentation of groundwater samples on the Durov diagram (Fig. 4) can be used to follow the geochemical evolutionary trend in the

Quaternary alluvial aquifer. This figure shows that the groundwaters from the downstream parts of Wadi Sudr and Wadi Wardan are plotted in the Mg-Cl field indicating mixed water type that is possibly evolved from Ca-HCO<sub>3</sub> recharge water, which on mixing with pre-existing groundwater and/or seawater yields Mg-SO<sub>4</sub> waters. The latter water type is further evolved to give Mg-Cl water type. Geochemical evolution proceeds, as indicated by the arrow on the Durov diagram, towards the Na-Cl type that is represented by sample # 12 (Ain Gharandal). Na-Cl water is considered as the end member of the groundwater geochemical evolution, which is consistent with the high salinity value of this sample.



**Fig. 4.** Durov plot of the groundwater samples showing water types and the geochemical evolutionary trend.

Ionic ratios of the groundwater samples collected from the coastal Quaternary aquifer were plotted against Cl concentrations to show their hydrogeochemical characteristics and the main geochemical processes leading to the current water quality (Fig. 5). Groundwater from the coastal Quaternary aquifer has values of HCO<sub>3</sub>/Cl ratio close to the seawater ratio indicating possible mixing with seawater, where groundwater becomes enriched in Cl that leads to decrease the value of this ratio. Most of the groundwater samples from the Quaternary aquifer have Na/Cl ratio less than that of seawater which may be attributed to

depletion of Na probably caused by cation exchange. This process is associated with saltwater intrusion in coastal aquifers. Two samples (8 and 12) have values close to that of seawater indicating mixing with saltwater which is consistent with the high salinity values of these samples. Values of Ca/Mg and Ca/Na are much more than those of seawater, which may be due to enrichment of Ca by dissolution of carbonate minerals in the aquifer matrix and/or depletion of Na caused by cation exchange during mixing with saltwater. Values of Ca/Mg molar ratio of the groundwater from the coastal Quaternary aquifer are close to one, which indicates either dolomite dissolution or Mg enrichment caused by mixing with seawater. Ca/SO<sub>4</sub> ratio is also exceeding that of seawater and approaching a value of 1.0 which is probably resulting from dissolution of sulfate minerals (gypsum and anhydrite) commonly found in the Quaternary aquifer matrix.

The Br/Cl ratio has been used to distinguish salinity of marine and non-marine origins (Andreasen and Fleck, 1997). Because Br and Cl are relatively conservative in hydrological systems, the Br/Cl ratios of fresh waters are primarily controlled by the initial ratio in precipitation. As sea salt spray is the primary source of these ions in precipitation in west Sinai coastal area, precipitation should have a Br/Cl ratio similar to that of seawater. Thus, the Br/Cl ratio should be constant when salinization of fresh water occurs by simple mixing of seawater if there is no anthropogenic contamination. On the bivariate plot of Br/Cl ratios vs. Cl, as Cl concentration increases, the Br/Cl ratios of groundwaters with high Cl concentrations are maintained in the normal seawater value of 0.00155, indicating that the salinization of these groundwaters results mainly from mixing with seawater and/or dissolution of marine aerosols rich in those elements. However, a slight decrease of the Br/Cl ratios in low-Cl samples is observed in Fig. 5. This probably results from anthropogenic Cl pollution because Cl contents of groundwaters in agricultural areas (commonly overly the Quaternary aquifer) can easily increase without an accompanying increase in Br contents. The I/Cl ratios of most of groundwaters are similar to or slightly less than that of seawater (Fig. 5), suggesting that their salinities mainly resulted from modern seawater.



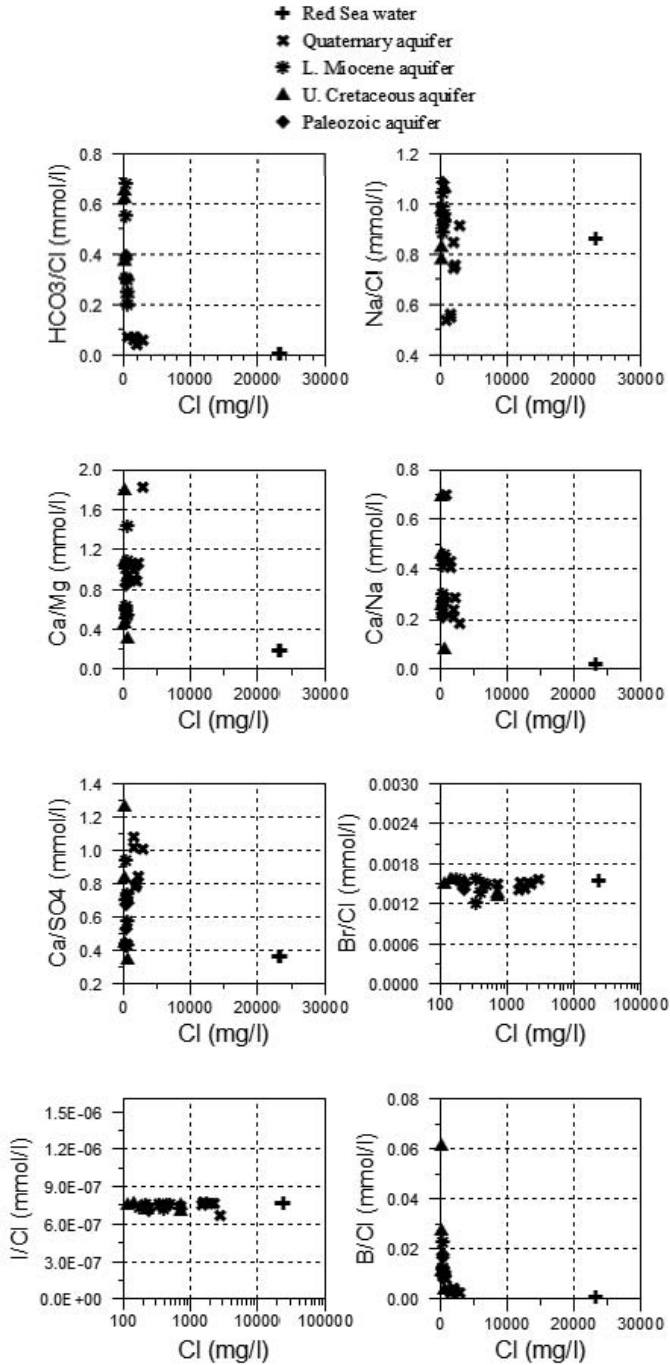


Fig. 5. Molar ratios of major and minor ion data for groundwaters from the study area.

Boron is generally a conservative element in groundwater systems, where it increases with direct seawater mixing (Swanberg *et al.*, 1984). However, B can be removed from the aqueous system by adsorption onto clay minerals (Palmer *et al.*, 1987). The B/Cl ratios of the groundwater are close to the seawater ratio which confirms the geochemical similarity between groundwater from the Quaternary aquifer and seawater.

#### *Groundwater from the Neogene Water-Bearing Formations*

Groundwaters of the Lower Miocene at Wadi Sudr (water point # 5 or Ain Abu Garad) and Wadi Gharandal (water points 13, 14, 15, 17, 18, and 19) are characterized by lower salinity values than those of the Quaternary aquifer. These groundwaters have pH values ranging from 7.28 to 7.65 indicating a near-neutral nature of the groundwater. TDS values vary between 755 and 2240 mg/l indicating that groundwater varies from fresh to brackish. The chemical facies of the groundwater from the Neogene water-bearing formations are shown in Table (2). These facies are characterized by the dominance of Na, followed by Ca and/or Mg. Magnesium is the dominant cation followed by Na and Ca in one sample (water point # 14). Anions show varying dominance in the chemical facies, however, Cl and SO<sub>4</sub> are the dominant anions, which show mutual dominance. As shown on Piper diagram (Fig. 3), all the groundwater samples are characterized by the dominance of Ca + Mg over Na and dominance of Cl + SO<sub>4</sub> over HCO<sub>3</sub>. Increase of Ca and SO<sub>4</sub> contents in groundwater is attributed to dissolution of gypsum and anhydrite which are commonly found in the Miocene formations of Wadi Gharandal.

Figure 4 shows the distribution of groundwater samples from the Neogene water-bearing formations on the Durov diagram. The samples are plotted in the Mg-SO<sub>4</sub> field and close to the border with the Mg-Cl water type reflecting a mixed water type resulting from mixing of Ca-HCO<sub>3</sub> recharge water with the groundwater in the Miocene formations.

Figure 5 shows that values of HCO<sub>3</sub>/Cl and Na/Cl ratios are exceeding that of seawater indicating different geochemical characteristics where dissolution/precipitation reactions and cation exchange are the prevailing processes responsible for the chemical composition of the groundwaters from the Miocene water-bearing formations. Values of Ca/Mg, Ca/Na and Ca/SO<sub>4</sub> ratios exceed that of sea water which is mainly attributed to dissolution of carbonate and

sulfate minerals occasionally found in the Lower Miocene formations. Values of Br/Cl and I/Cl ratios are slightly less than and close to the seawater ratios, which suggests dissolution of marine aerosols. Values of B/Cl ratio indicate enrichment of groundwaters with B, which is mainly derived from clays that are commonly found in clastics of the Miocene formations.

#### *Groundwater from the Upper Cretaceous-Eocene Karstified Limestone Aquifer*

The karstic groundwaters from the upper part of Wadi Sudr (water points from 1 to 4) and the lower part of Wadi Abu Gaada (water point # 16 or WGH-5) show water salinities vary from fresh to brackish. The groundwaters have a near neutral to slightly alkaline pH (ranges from 7.43 to 8.33), where slight increase of pH values could be attributed to dissolution of carbonate minerals. TDS values range from 538 mg/l at water point # 3 (Ain Henaik) to 2445 mg/l at Ain Abu Rejem in the upper part of Wadi Sudr. High salinity values reflect the extent of water-rock interactions where dissolution of carbonate rocks is an active process in such karstified systems. These waters have varying chemical facies (Table 2). Sodium is mostly the dominant cation followed by Ca and/or Mg in the groundwater discharged from Wadi Sudr springs. Calcium is the dominant cation followed by Na in groundwater discharged from Ain Henaik in Wadi Sudr. However, Ca is not represented in the chemical facies of groundwater from Ain Sudr (water point # 1) and Ain Abu Rejem (water point # 2), which are characterized by the highest TDS values. Chloride is the dominant anion followed mostly by  $\text{SO}_4$  in groundwater from Wadi Sudr springs, whereas the reverse is the case for groundwater from WGH-5 (water point # 16) in Wadi Abu Gaada. The latter groundwater has Mg as the dominant cation followed by Na, whereas Ca is absent in its chemical facies. As illustrated by the Piper diagram (Fig. 3), the cation evolution of the karstified groundwater is mainly characterized by enrichment of either Na or Ca and Mg. Chloride and sulfate are the characteristic anions in all groundwaters from the karstified limestone aquifers in Wadi Sudr and Wadi Abu Gaada.

Geochemical evolution of groundwaters can be traced on the Durov's diagram (Fig. 4) where the karstified groundwaters are initially recharged by Ca- $\text{HCO}_3$  water (rain water) and undergo water-rock interactions (dissolution-precipitation) and mixing with pre-existing groundwater in the karstified limestone that may be of saline nature. This

leads to the evolution of Mg-SO<sub>4</sub> (Ain Henaik, Ain Um Gorf) and Mg-Cl (Ain Abu Rejem) water types and finally reach an advanced state of geochemical evolution, which is represented by the Na-Cl type (Ain Sudr).

Geochemical characteristics of groundwaters from the karstified limestone can be explained through discussion of the commonly used ionic ratios plotted against Cl contents (Fig. 5). Values of HCO<sub>3</sub>/Cl ratio show enrichment of karstified groundwater with HCO<sub>3</sub> relative to seawater which can be attributed to dissolution of carbonate rocks composing the aquifer matrix. Na/Cl ratio shows that groundwaters from Ain Henaik and Ain Um Gorf are depleted in Na leading to decrease of the ratio. Depletion of Na may be due to less Na source in the aquifer matrix and/or cation exchange through clastics (mainly clays) and marly limestone of the Lower Eocene-Paleocene Esna Formation. Ca/Mg, Ca/Na and Ca/SO<sub>4</sub> ratios show enrichment of groundwaters with Ca that is mainly resulting from dissolution of carbonate rocks. However, groundwater from Ain Sudr has the lowest values of these ratios, which indicates that this groundwater is depleted in Ca. This can be attributed to mixing with residual saltwater rich in Mg rather than dissolution of dolomitic limestone in the karstified formations which is consistent with high salinity and the Na-Cl chemical facies of Ain Sudr. This is because dissolution of dolomite yields groundwater with a Ca/Mg molar ratio of 1.00. Figure (5) shows that Br/Cl and I/Cl are slightly less than and close to the seawater ratio. This can be attributed to dissolution of marine aerosols (Winchester and Duce, 1967). Therefore, dissolution and evaporative concentration of marine aerosols in the elevated recharge area may yield significant Br concentrations in groundwater, and this could be the source for much of NaCl in the groundwaters as well. Therefore, values of Br/Cl and I/Cl ratios remain close to those of seawater. Clays and marly limestones in the aquifer matrix play an important role in controlling B contents in groundwater of the karstified Upper Cretaceous aquifer, which is reflected in the higher values of B/Cl ratio.

#### *Groundwater from the Paleozoic Water-Bearing Formations*

Groundwater from the Cambrian (water point # 20) and Carboniferous (water point # 21) water-bearing formations are mainly fresh water with TDS values of 928 and 832 mg/l, respectively. These groundwaters have pH values of 7.30 and 7.12, respectively, indicating a

near-neutral nature. The groundwater hydrochemical facies are characterized by the dominance of Na, which is followed by Mg in groundwater from the Cambrian water-bearing formation (Arabah Formation), whereas Mg is not represented in that of the Carboniferous water-bearing formation (Abu Thora Formation). Chloride and  $\text{SO}_4$  are the dominant anions in the two chemical facies. Plots of these two samples on Piper diagram (Fig. 3) show that the groundwater from the Cambrian aquifer is characterized by dominance of Ca + Mg over Na, whereas the reverse is characteristic for the groundwater from the Carboniferous aquifer. The two samples show dominance of Cl +  $\text{SO}_4$  over  $\text{HCO}_3$ .

The groundwaters of the Paleozoic water-bearing formations are plotted in the Mg- $\text{SO}_4$  field of the Durov diagram (Fig. 4) indicating a mixed water type possibly evolved from the Ca- $\text{HCO}_3$  recharge rain water falling on the elevated tableland (El Tih plateau) located to the north of the Paleozoic water-bearing formations.

Values of  $\text{HCO}_3/\text{Cl}$  and  $\text{Na}/\text{Cl}$  ratios are exceeding those of seawater reflecting meteoric origin of the groundwater (Fig. 5). Enrichment of groundwater with  $\text{HCO}_3$  is attributed to dissolution of carbonate rocks dominating in the recharge area (El Tih plateau), which is mainly composed of Eocene and Cretaceous carbonate rocks. Ca/Mg, Ca/Na and Ca/ $\text{SO}_4$  ratios indicate that groundwaters are enriched in Ca, which is also due to dissolution of carbonate rocks in the recharge area. Values of the Br/Cl and I/Cl ratios are nearly close to the seawater ratios. Br and I contents in such inland fresh groundwaters are mainly derived from dissolution of marine aerosols falling on the elevated recharge area. Values of B/Cl ratio are exceeding that of sea water, where clays in the sandstone aquifers are the possible source of B.

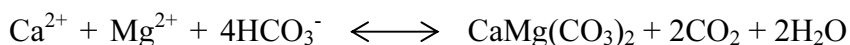
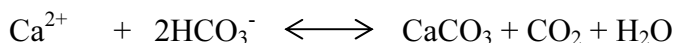
### ***Solution–Mineral Equilibria***

The saturation indices of some common carbonate (aragonite, calcite and dolomite) and sulfate (gypsum and anhydrite) minerals are shown in Fig. 6.

Most of the groundwaters from the Quaternary alluvial aquifer at the downstream parts of Wadi Sudr and Wadi Wardan are slightly to moderately oversaturated with respect to the carbonate minerals (aragonite, calcite and dolomite) indicating their precipitation in the aquifer matrix. Agricultural return flow results in dissolution of the

sparingly soluble carbonate minerals, which precipitate in the soil zone due to high evaporation rate. This will lead to increase the saturation states of these minerals in the underlying groundwater. Few samples are under-saturated with respect to carbonate minerals indicating that these minerals can dissolve by the aggressive groundwater. The groundwaters are also slightly under-saturated with respect to sulfate minerals (gypsum and anhydrite) indicating that more sulfate minerals will dissolve to increase their saturation states.

The Ca contribution from the cation exchange, the Mg increase due to seawater intrusion as well as the  $\text{HCO}_3^-$  increase from dissolution of carbonate minerals affect the carbonate equilibria causing supersaturation with regard to calcite and/or dolomite according to:



To check this assumption, the saturation indices (SI) have been calculated for carbonate minerals (Fig. 6). For most of the samples, the SI of calcite and dolomite are close to or above 0. Thus, dolomite or magnesian calcite precipitation is likely to occur in the Quaternary aquifer.

The groundwaters from the Lower Miocene formations in Wadi Sudr and Wadi Gharandal vary between slight under-saturation to near saturation with respect to carbonate minerals which is consistent with the clastic nature of the Miocene formations. They are also moderately to strongly undersaturated with respect to sulfate minerals indicating that these minerals can dissolve to yield more Ca and  $\text{SO}_4$  to the groundwater.

The groundwaters from the Upper Cretaceous-Eocene highly fractured and karstified limestone aquifer are mostly slightly to strongly over-saturated with respect to the common carbonate minerals (aragonite, calcite and dolomite) indicating that these minerals are susceptible to precipitation in the aquifer matrix. This is consistent with the karstified nature of the limestone where dissolution is the prominent process. Groundwater from the Upper Cretaceous aquifer in Wadi Gharandal is slightly under-saturated with respect to carbonate minerals indicating that their dissolution is possible. The groundwaters are strongly under-saturated with respect to sulfate minerals (gypsum and anhydrite) indicating the possibility of their dissolution through water-rock interaction.

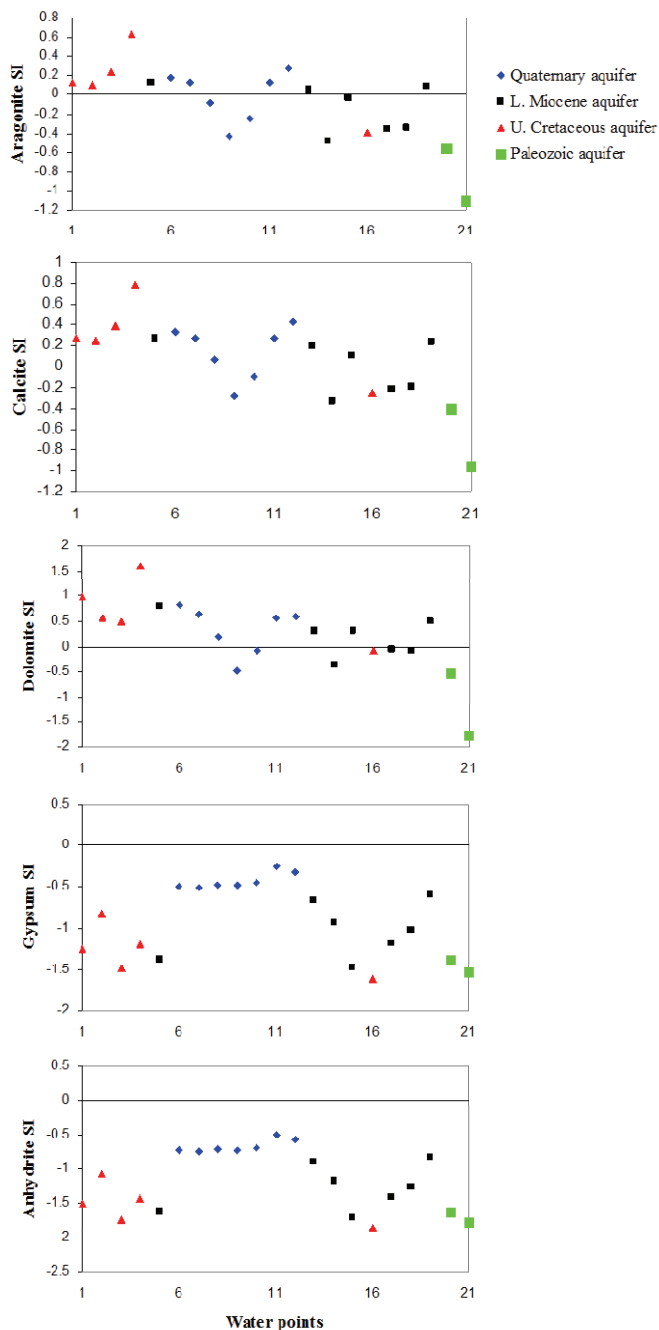


Fig. 6. Saturation indices of the common carbonate and sulfate minerals in the collected groundwater samples.

The groundwaters from the Cambrian and Carboniferous water-bearing formations are moderately to strongly undersaturated with respect to the carbonate and sulfate minerals. This is consistent with the lithology of these formations, which is mainly sandstones lacking carbonate and sulfate minerals.

### *Isotopic Characterization*

Isotopic measurements were carried out on groundwaters from the different aquifers in the study area. The  $^{18}\text{O}$  and  $^2\text{H}$  contents of these groundwaters are shown in Fig. (7) and are reported in Table (1).

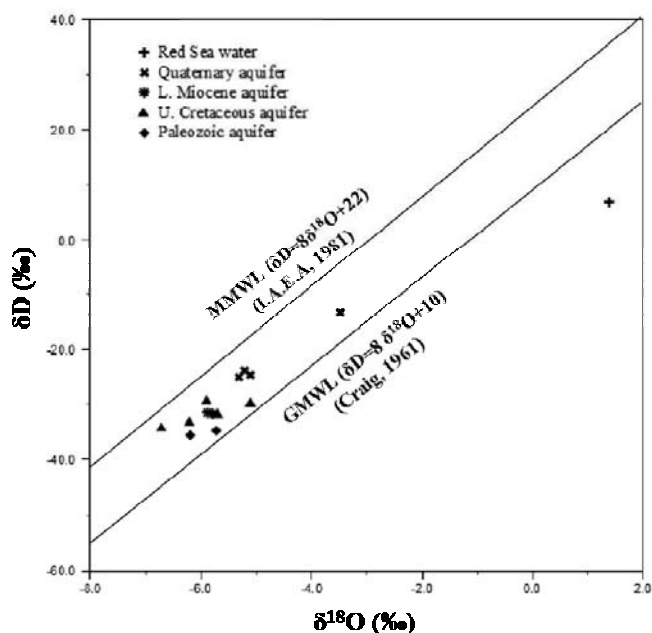


Fig. 7. The  $\delta\text{D}-\delta^{18}\text{O}$  relation for the groundwater samples collected from the study area. The Global Meteoric Water Line (GMWL) and Mediterranean Meteoric Water Line (MMWL) are also shown.

The groundwater collected from the different water-bearing formations at the Ras Sudr-Abu Zenima area are depleted in  $^2\text{H}$  and  $^{18}\text{O}$ , where the isotopic contents vary between -35.7 and -13.6‰ and between -6.7 and -3.49‰, respectively. The relationship between  $\delta^2\text{H}$  and  $\delta^{18}\text{O}$  shows that groundwater samples display an isotopic signature close to that of meteoric water, where they plot just above the global meteoric water line (GMWL),  $\delta^2\text{H} = 8 \delta^{18}\text{O} + 10$ , given by Craig (1961) with d-



excess value of 10%. Furthermore, the plots representing groundwaters from the study area fall below the local eastern Mediterranean meteoric water line (MMWL),  $\delta^2\text{H} = 8 \delta^{18}\text{O} + 22$ , given by Gat *et al.* (1969) and IAEA (1981). This line represents modern Mediterranean precipitation enriched in  $^2\text{H}$  with d-excess value of 22%. This corresponds to present-day precipitation over the region and reflects the contribution of vapour masses from Mediterranean origin. Groundwaters collected from the study area show a deuterium excess (d-excess =  $\delta^2\text{H} - 8 \delta^{18}\text{O}$ ) higher than 10% (ranges from 10.96 to 19.4%) (Table 1). These isotopic features suggest that most of the groundwaters results from a mixing between recent recharge and an older component recharged under climatic conditions cooler than at present.

Groundwaters from the study area show nearly similar isotopic compositions suggesting similar recharge conditions. However, groundwaters from the Quaternary alluvial aquifer are slightly enriched with  $^2\text{H}$  and  $^{18}\text{O}$ . This is clear from the plot of the groundwater sample collected from Ain Gharandal (water point # 12), which is the nearest one to the point representing sea water. Enrichment with heavy isotopes of hydrogen and oxygen indicates possible mixing of groundwater with salt water. Moreover, groundwaters from the Cambrian and Carboniferous water-bearing formations show d-excess values of 13.9 and 10.96%, respectively, which indicates that older component of recharge is prevailing than the recent one.

### Conclusions

The hydrogeochemical and isotopic investigation of the groundwater from the different water-bearing formations of the Ras Sudr-Abu Zenima area, southwest Sinai, Egypt reveals that the groundwater results from mixing between Ca-HCO<sub>3</sub> recharge water falling on the elevated tableland (El-Tih plateau) and the pre-existing groundwater to yield mixed water of the Mg-SO<sub>4</sub> and Mg-Cl types. These water types undergo further geochemical evolution through water-rock interaction and/or mixing with seawater to reach a final stage of evolution represented by the Na-Cl water type. The coastal Quaternary alluvial aquifer shows the highest salinity values and predominance of Na and Cl in the groundwater chemical facies. The groundwater of the Quaternary aquifer has molar ratios of Br/Cl, I/Cl and B/Cl that are nearly close to the seawater ratio and this indicates the contribution of

seawater. Cation exchange reactions during seawater intrusion increase Ca and Mg contents in the water, whereas dissolution of carbonate minerals in the recharge area increases Ca, Mg and HCO<sub>3</sub> contents. Moreover, simple mixing with seawater causes high Mg contents in groundwater. The increase of Ca, Mg and HCO<sub>3</sub> shifts the carbonate equilibrium and leads to dolomite and/or magnesian calcite precipitation. Isotopic signature of groundwater from the different water-bearing formations indicated the meteoric origin of groundwater due to present-day precipitation over the region and reflects the contribution of vapour masses from Mediterranean origin. Values of deuterium excess of the groundwater from the Cambrian and Carboniferous water-bearing formations (13.9 and 10.96%, respectively) indicated that older component of recharge is prevailing than the recent one.

### ***Acknowledgements***

The author wishes to express his sincere appreciation to Dr. Rifai I. Rifai for carrying out the stable isotope analyses at the National Center, U.S. Geological Survey, Reston, USA, and Dr. Milad H. Masoud for the analysis of Br and I at the Desert Research Center, Cairo, Egypt.

### **References**

- Abdallah, A. M., Darwish, M., El Aref, M. and Helba, A. A.** (1992) Lithostratigraphy of the Pre-Cenomanian clastics of north Wadi Qena, Eastern Desert, Egypt. *Proceedings of the First International Conference on Geology of the Arab World*, Cairo University, Cairo: 255-282.
- Abdel-Mogheeth, S.M., Hammad, F.A. and Abdel-Daiem, A.A.** (1985) hydrogeological remarks on Gharandal Basin, southwest Sinai Peninsula. *Desert Inst. Bull.*, Egypt, **5** (2): 309-329.
- American Public Health Association (APHA)**, 1998. *Standard Methods for the Examination of Water and Wastewater*, 20<sup>th</sup> ed. American Public Health Association, Washington, USA.
- Andreasen, D.C. and Fleck, W.B.** (1997) Use of bromide:chloride ratios to differentiate potential sources of chloride in a shallow, unconfined aquifer affected by brackish-water intrusion. *Hydrogeol. J.*, **5**: 17–26.
- Appelo, C.A.J. and Postma, D.** (2005) *Geochemistry, Groundwater and Pollution*. 2<sup>nd</sup> Edition, Balkema, Rotterdam.
- Barbieri, M., Boschetti, T., Pettita, M. and Tallini, M.** (2005) Stable isotope (<sup>2</sup>H, <sup>18</sup>O and <sup>87</sup>Sr/<sup>86</sup>Sr) and hydrochemistry monitoring for groundwater hydrodynamics analysis in a karst aquifer (Gran Sasso, Central Italy). *Appl. Geochem.*, **20**: 2063–2081.
- Capacciona, B., Diderob, M., Palettab, C. and Didero, L.** (2005) Saline intrusion and refreshing in a multilayer coastal aquifer in the Catania Plain (Sicily, Southern Italy): dynamics of degradation processes according to the hydrochemical characteristics of groundwaters. *J. Hydrol.*, **307**: 1–16.

- Cardona, A., Carrillo-Rivera, J.J., Huizar-Alvarez, R. and Graniel-Castro, E.** (2004) Salinization in coastal aquifers of arid zones: an example from Santo Domingo, Baja California Sur, Mexico. *Environ. Geol.*, **45**: 350–366.
- Clark, I. and Fritz, P.** (1999) *Environmental Isotopes in Hydrogeology*. Lewis Publishers, New York.
- Cook, P.G. and Herczeg, A.L.** (1999) *Environmental Tracers in Subsurface Hydrology*. Kluwer Academic Press, Boston, MA.
- Conoco** (1987) *Geological Map of Egypt* (scale 1 : 500,000, NH 36 NE South Sinai and NH 36 SW Beni Suef).
- Coplen, T.B., Wildman, J.D. and Chen, J.** (1991) Improvements in the gaseous hydrogen-water equilibration technique for hydrogen isotope ratio analysis. *Analytical Chemistry*, **63**: 910–912.
- Craig, H.** (1961) Isotopic variations in meteoric waters. *Science*, **133**: 1702–1703.
- Craig, H.** (1969) Geochemistry and Origin of the Red Sea Brines. In: E.T. Degens and D.A. Ross, (ed.) *Hot Brines and Recent Heavy Metal Deposits in the Red Sea*, Springer Verlag, New York: 208–242.
- Custodio, E.** (1987) Hydrogeochemistry and tracers. In: Custodio, E. (Ed.), *Groundwater Problems in Coastal Areas*. Studies and Reports in Hydrology, UNESCO, Paris, **45**: 213–269.
- Egyptian General Petroleum Corporation EGPC** (1964) Oligocene and Miocene rock stratigraphy of the Gulf of Suez region. *Report of the Stratigraphic Committee*, 142 p.
- El Baruni, S.** (1995) Deterioration of the quality of groundwater from Suani wellfield, Tripoli, Libya. *Hydrogeol. J.*, **3**: 58–64.
- E1-Gammal, R.M.H.** (1984) Geological studies on the stratigraphic succession of Umm Bogma district, west central Sinai, Egypt. *M.Sc. Thesis*. Cairo University, Egypt, 180 p.
- El Mandour, A., El Yaouti, F., Fakir, Y., Zarhloule, Y. and Benavente, J.** (2007) Evolution of groundwater salinity in the unconfined aquifer of Bou-Areg, Northeastern Mediterranean coast, Morocco. *Environ. Geol.*, **54**: 491–503.
- El Sayed, E., Ismail, Y. L. and Gomaa, M. A.** (1999) Hydrogeological investigation in the coastal area of the delta of Wadi Sudr, Gulf of Suez, south Sinai, Egypt. *Bull. Fac. Sci., Assiut Univ.*, **28** (2-F): 143–160.
- Epstein, S. and Mayeda, T.** (1953) Variation of  $^{18}\text{O}$  content of water from natural sources. *Geochim. Cosmochim. Acta*, **4**: 213–224.
- Ferrara, V. and Pappalardo, G.** (2004) Intensive exploitation effects on alluvial aquifer of the Catania plain, eastern Sicily, Italy. *Geofisica Internazionale*, **43**: 671–681.
- Gat, J.R., Mazor, E. and Tzur, Y.** (1969). The stable isotope composition of mineral waters in the Jordan Rift Valley, Israel. *J. Hydrology*, **76**: 334–352.
- Gawad, W.A., Gaafar, I. and Sabour, A.A.** (1986). Miocene stratigraphic nomenclature in the Gulf of Suez region. *Egyptian General Petroleum Corporation 8<sup>th</sup> Exploration Conference*: 1–20.
- Ghorab, M. A.** (1961) Abnormal stratigraphic features in Ras Gharib oilfield. *Third Arab Petroleum Congress, Alexandria*: 1–10.
- Grassi, S. and Netti, R.** (2000) Sea water intrusion and mercury pollution of some coastal aquifers in the province of Grosseto (Southern Tuscany, Italy). *J. Hydrol.*, **237**: 98–211.
- Hassanein, A. H.** (1989) Geology of water resources in Wadi Sudr-Wadi Gharandal area, Gulf of Suez region, Sinai Peninsula, Egypt. *M. Sc. Thesis*, Fac. Sc., Ain Shams Univ., Cairo.
- Herrera, L.M., Espinosa, J.R., Millán, J.J. and Hiscock, K.M.** (2008) Integrated hydrochemical assessment of the Quaternary alluvial aquifer of the Guadalquivir River, southern Spain. *Applied Geochemistry*, **23**: 2040–2054.
- I.A.E.A.** (1981) Stable isotope hydrology. Deuterium and oxygen-18 in water cycle. In: J.R. Gat, and R. Gonfiantini, (ed.), *International Atomic Energy Agency Technical Report No. 210, Vienna*, 339 p.

- Issar A., Bein, A. and Michael, A.** (1972) On the ancient water of the upper Nubian Sandstone aquifer in central Sinai and southern Israel. *Hydrogeol. J.*, **17**:353-374
- Issawi, B.** (1973) Review of Upper Cretaceous-Lower Tertiary Stratigraphy in central and southern Egypt. *American Association of Petrol. Geol. Bull.*, **56**(8): 1448-1463.
- Lambrakis, N.J., Voudouris, K.S., Tiniakos, L.N. and Kallergis, G.** (1997) Impact of simultaneous action of drought and overpumping on Quaternary aquifers of Glafkos basin (Patras region, western Greece). *Environ. Geol.*, **29**: 209–215.
- Long, A.J. and Putnam, L.D.** (2004) Linear model describing three components of flow in karst aquifers using  $^{18}\text{O}$  data. *J. Hydrol.*, **296**: 254–270.
- Marfia, A.M., Krishnamurthy, R.V., Atekwana, E.A. and Panton, W.F.** (2003) Isotopic and geochemical evolution of ground and surface waters in a karst dominated geological setting: a case study from Belize, Central America. *Appl. Geochem.*, **19**: 937–946.
- Melloul, A.** (1995) Use of principal components analysis for studying deep aquifers with scarce data-application to the Nubian Sandstone aquifer, Egypt and Israel. *Hydrogeol. J.*, **3**(2):19-39.
- Mills, A. C. and Shata, A.** (1989) Ground-water assessment of Sinai, Egypt. *Ground Water*, **27** (6): 793-801.
- Misak, R. F., Atwa, S. M., Sallouma, M. K. and Hassanein, A. H.** (1995) Geology and water quality of the groundwater supplies in Sudr-Gharandal area, Gulf of Suez, Egypt. *Bull. Fac. Sci., Assiut Univ.*, **24** (2-F): 1-21.
- Omara, S.** (1967) Contribution to the stratigraphy of the Egyptian Carboniferous exposures.  $6^{\text{th}}$  Arab Petroleum Congress Baghdad **44**: 1-7.
- Palmer, M.R., Spivack, A.J. and Edmond, J.M.** (1987) Temperature and pH controls over isotopic fractionation during adsorption of boron on marine clay. *Geochim. Cosmochim. Acta*, **51**:2319-2323.
- Parkhurst, D.L. and Appelo, C.A.J.** (1999) *User's Guide to PHREEQC (version 2)—A Computer Program for Speciation, Batch-reaction, one-Dimensional Transport, and Inverse Geochemical Calculations*. USGS Water-Resources Investigations Report 99–4259.
- Petalas, C.P. and Diamantis, I.B.** (1999) Origin and distribution of saline groundwaters in the upper Miocene aquifer system, coastal Rhodope area, Northeastern Greece. *Hydrogeol. J.*, **7**: 305–316.
- Purser, B.H., Orszag-Sperber, F., Plaziat J.C. and Rioual, M.** (1993) *Plioquaternary Tectonics and Sedimentation in the Sw Gulf of Suez and N. Red Sea*. In: Thorweihe and Schandelmeier (Eds.) Geoscientific, A. A. Balkema, Rotterdam: 259-262.
- Said, R.** (1962): *The Geology of Egypt*. Elsevier, Amsterdam, 377p
- Said, K.** (1971) Explanatory note to accompany the geological map of Egypt. *Geologic Survey Egypt*, **56**:123 p.
- Salem, A.M.** (1995) Diagenesis and isotopic study of the Paleozoic clastic sequence (Cambrian and Carboniferous), southwest Sinai. *Ph. D. Thesis*. Tanta University, Egypt, 246p.
- Schütz, K.I.** (1994) Structure and stratigraphy of the Gulf of Suez, Egypt. In: Landon, S.M. (Ed.), *Interior Rift Basins*, AAPG Memoir 59, The American Association of Petroleum Geologists, Tulsa, Oklahoma, USA: 57-96.
- Sidle, W. C.** (1998) Environmental isotopes for resolution of hydrology problems. *Environ. Monitor. Assess.*, **52**: 389–410.
- Stamatis, G. and Voudouris, K.** (2003) Marine and human activity influences on the groundwater quality of southern Korinthos area (Greece). *Hydrol. Process.* **17**: 2327–2345.
- Swanberg, C.A., Morgan, P. and Boulos, F.K.** (1984) Geochemistry of the groundwaters of Egypt. *Annals of the Geol. Surv. Egypt*, **XIV**: 127-150.

- Water Resources Research Institute and Japan International Cooperation Agency** (1999). *South Sinai Groundwater Resources Study in the Arab Republic of Egypt*. Main Rep, WRRI, El-Kanater El Khayria.
- Wilson, T.R.S.** (1975) Salinity and Major Elements of Sea Water. In: J.P. Riley and G. Skirrow, (ed.) *Chemical Oceanography*, 2<sup>nd</sup> edition, Academic Press, London, New York, **1**: 365-413.
- Winchester, J.W. and Duce, R.A.** (1967) The global distribution of iodine, bromine, and chlorine in marine aerosols. *Naturwissenschaften*, **54**: 110-113.

## الخصائص الهيدروجيوكيميائية وتطور المياه الجوفية في منطقة رأس سدر - أبو زنيمة، جنوب غرب سيناء، مصر

أنور عبد العزيز الفقي

قسم جيولوجيا المياه - كلية علوم الأرض - جامعة الملك عبدالعزيز

جدة - المملكة العربية السعودية

المستخلص. تم دراسة البيانات الهيدروجيوكيميائية والنظائر للمياه الجوفية من المكونات المائية المختلفة في منطقة رأس سدر - أبو زنيمة، جنوب غرب سيناء، مصر، لمعرفة العوامل الأساسية التي تحكم كيمياء المياه الجوفية والملوحة وكذلك التطور الهيدروجيوكيميائي. تتواجد المياه الجوفية في مكونات مائية تنتمي للحقب الرباعي، والنيوجين، والطباشيري العلوي، وحقب الحياة القديمة. تم استخدام طرق مختلفة للتفسير الجيوكيميائي لمعرفة الخصائص الجيوكيميائية. تتميز المياه الجوفية بالخران الطميي الرباعي الساحلي بأعلى قيم للملوحة (2739 - 7040 مجم/لتر) في منطقة الدراسة بسبب تأثير مياه البحر والأنشطة الزراعية. ويوضح شكل بايير أن Cl و SO<sub>4</sub> هما الأنيونات السائدة بينما Na هو أكثر الكاتيونات سيادة و الذي في بعض الأحيان يستبدل بـ Ca و/أو Mg في السحنات الهيدروجيوكيميائية للمياه الجوفية. وقد أثبت شكل ديوروف أن المياه الجوفية تطورت من مياه التغذية ذات النوع Ca-HCO<sub>3</sub> عن طريق امتزاجها مع المياه الجوفية الموجودة لتعطي مياهًا مختلطة من نوع Mg-SO<sub>4</sub> و Mg-Cl والتي تصل في النهاية إلى المرحلة النهائية للتطور والمثلة بنوع مياه Na-Cl. أثبتت النسب الأيونية المختلفة تأثير مياه البحر والرذاذ البحري على

التركيب الهيدروكيميائي للمياه الجوفية في المتكون المائي التابع للحقب الرباعي. وقد أوضحت عمليات إذابة معادن الكربونات والكبريتات في المتكونات المائية ومنطقة التغذية وكذلك عملية تبادل الكاتيونات أنها تعدل تركيزات الأيونات في المياه الجوفية.

وقد أوضحت عمليات الاتزان بين المياه الجوفية والمعادن تفاعلات الإذابة والترسيب السائدة في المياه الجوفية. ووجد أن المياه الجوفية مستنزفة بالنسبة لنظائر  $^2\text{H}$  و  $^{18}\text{O}$ ، وهذا يشير إلى بصمة نظائر قريبة لبصمة المياه الجوية والتي لها قيم d-excess تدل على تساقط حديث على المنطقة والذي يعكس مساهمة كتل بخار الماء ذات نشأة من البحر المتوسط. ويمكن من خصائص النظائر اقتراح أن معظم المياه الجوفية في منطقة الدراسة قد نتجت من امتزاج مياه التغذية الحديثة مع مياه التغذية القديمة، والتي حدثت في ظروف جوية أبرد من الظروف الحالية. علاوة على ذلك فإن المياه الجوفية من المتكونات التابعة لعصري للكامبري والكربوني ذات قيم d-excess 13,9، و 10,96% على التوالي والتي تدل على أن مياه التغذية القديمة هي السائدة أكثر من مياه التغذية الحديثة. وتدل بصمة النظائر في المياه الجوفية من المتكون المائي التابع للحقب الرباعي على مساهمة مياه البحر.